Journal of Power Sources 193 (2009) 828–833

Contents lists available at ScienceDirect

Journal of Power Sources

journal homepage: www.elsevier.com/locate/jpowsour

Influence of synthesis conditions on electrochemical properties of high-voltage $Li_{1.02}Ni_{0.5}Mn_{1.5}O_4$ spinel cathode material

B.J. Hwang[a,b,*], Y.W. Wu[a], M. Venkateswarlu[a], M.Y. Cheng[a], R. Santhanam[c]

[a] Nanoelectrochemistry Laboratory, Department of Chemical Engineering, National Taiwan University of Science and Technology, 43 Keelung Road, Section 4, Taipei 106, Taiwan
[b] National Synchrotron Radiation Research Center, Hsinchu 300, Taiwan
[c] Nanoexa Corporation, Burlingame, CA, USA

ARTICLE INFO

Article history:
Received 16 December 2008
Received in revised form 19 March 2009
Accepted 13 April 2009
Available online 22 April 2009

Keywords:
Cathode
Spinel
Li-ion battery
High-voltage

ABSTRACT

$Li_{1.02}Ni_{0.5}Mn_{1.5}O_4$ spinel cathode materials were successfully synthesized by a citric acid-assisted sol–gel method. The structure and morphology of the materials have been examined by X-ray diffraction and scanning electron microscopy, respectively. Electrochemical properties of the materials were investigated using cyclic voltammetry and galvanostatic charge/discharge measurements at two different temperatures (25 and 55 °C) using lithium anode. The initial capacity and capacity retention are highly dependent on the particle size, particle size distribution, crystallinity and purity of the materials. The $Li_{1.02}Ni_{0.5}Mn_{1.5}O_4$ materials synthesized both at 800 and 850 °C have shown best electrochemical performance in terms of capacity and capacity retention between 3.5 and 4.9 V with a $LiPF_6$ based electrolyte.

© 2009 Elsevier B.V. All rights reserved.

1. Introduction

Rechargeable lithium-ion batteries have become dominant power sources for portable electronic devices and implantable medical applications. They are now considered to be the technology of choice for future hybrid electric and electric vehicles to address global warming [1–3]. Layered transition metal oxides such as $LiCoO_2$ and $LiNiO_2$ and spinel oxide $LiMn_2O_4$ are the most important materials for use as cathode materials in lithium-ion batteries [4–6]. Among these materials, $LiMn_2O_4$ is currently a very promising cathode material, especially for large sized batteries for electric vehicle applications, due to its low cost, abundance and non-toxicity and has been studied extensively [7–10]. However, $LiMn_2O_4$ exhibits severe capacity fading on cycling mainly due to dissolution of Mn in to the electrolyte via the disproportionation reaction: $2Mn^{3+} \rightarrow Mn^{2+} + Mn^{4+}$ and Jahn–Teller distortion of trivalent Mn ions [11–13]. Therefore, various attempts have been made to enhance the cycling stability of the spinel $LiMn_2O_4$.

One effective approach to improve the cycling performance is partial substitution of manganese by other dopant ions to make $LiM_xMn_{2-x}O_4$ (M = Al, Ni, Co, Fe, Cr, etc) [14–19]. It has been reported that all these substitutions show a slightly decreased capacity in the 4 V plateau but enhances the cycling performance significantly. The discharge capacities and the voltage plateaus strongly depend on the nature of the dopants and their content. Among all possible compositions, $LiNi_{0.5}Mn_{1.5}O_4$ is the most attractive material because of its high discharge capacity (>130 mAh g^{-1}) and flat plateau at 4.7 V whereas other materials have showed two plateaus at around 4 and 5 V [16]. In addition, this material has been demonstrated to show good cycling stability on lithium on extraction and insertion and good rate capability [20–23]. $LiNi_{0.5}Mn_{1.5}O_4$ spinel material is fundamentally different from pure Mn spinels as all the redox activities occur entirely at the on Ni^{2+} ion while the Mn^{4+} remains as structure stabilizing ion during charging and discharging [24]. Ohzuku's group have published a series of research papers on $LiNi_{0.5}Mn_{1.5}O_4$ spinel and also successfully demonstrated a 3 V lithium-ion cell with $LiNi_{0.5}Mn_{1.5}O_4$ spinel and the zero-strain insertion material $Li[Li_{1/3}Ti_{5/3}]O_4$ and the cell showed a quite flat operating voltage of 3.2 V with excellent cycleability [25–28].

In general, $LiNi_{0.5}Mn_{1.5}O_4$ was synthesized by conventional solid-state method [29,30]. However, this method requires an extensive mechanical mixing of lithium hydroxide or carbonates or nitrates with manganese followed by high temperature grinding. Moreover, $LiNi_{0.5}Mn_{1.5}O_4$ spinel material prepared by solid-state reaction produces larger particles of irregular shape and poor control of stoichiometry. All these problems could be eliminated or minimized by employing liquid phase synthesis process such as sol–gel or modified sol–gel process under controlled conditions. Sol–gel process can produce highly homogeneous

* Corresponding author at: Nanoelectrochemistry Laboratory, Department of Chemical Engineering, National Taiwan University of Science and Technology, 43 Keelung Road, Section 4, Taipei 106, Taiwan. Tel.: +886 2 27376624; fax: +886 2 27376644.
E-mail address: bjh@mail.ntust.edu.tw (B.J. Hwang).

0378-7753/$ – see front matter © 2009 Elsevier B.V. All rights reserved.
doi:10.1016/j.jpowsour.2009.04.012

Table 1
Lattice parameters for the $Li_{1.02}Ni_{0.5}Mn_{1.5}O_4$ synthesized at various temperatures.

Sample	Lattice parameter (a)	Cell volume (Å^3)
$Li_{1.02}Ni_{0.5}Mn_{1.5}O_4$ (700 °C)	8.1708	545.4987
$Li_{1.02}Ni_{0.5}Mn_{1.5}O_4$ (750 °C)	8.1699	545.3185
$Li_{1.02}Ni_{0.5}Mn_{1.5}O_4$ (800 °C)	8.1643	544.1979
$Li_{1.02}Ni_{0.5}Mn_{1.5}O_4$ (850 °C)	8.1695	545.2384

smaller particles with a narrow particle size distribution and good crystallinity [14,31]. Hence, the material synthesized by sol–gel method is expected to have enhanced electrochemical performance.

In this present work, the spinel $Li_{1.02}Ni_{0.5}Mn_{1.5}O_4$ has been synthesized by citric acid-assisted sol–gel process, which can solve the disadvantages of the conventional synthesis methods. The extra lithium is used in this material to push the manganese away from trivalent to tetravalent, thus minimizing the impact of any Jahn–Teller distortion coming from Mn^{3+}. The effect of sintering temperature on the particle morphology and electrochemical properties of $Li_{1.02}Ni_{0.5}Mn_{1.5}O_4$ spinel is discussed. To clarify the structure and morphology of $Li_{1.02}Ni_{0.5}Mn_{1.5}O_4$ spinel material prepared by citric acid-assisted sol–gel process under different conditions and their relationships with electrochemical performance, the samples are characterized by X-ray diffraction (XRD), scanning electron microscopy (SEM) and cyclic voltammetry (CV). The electrochemical lithium insertion and deinsertion properties of the $Li_{1.02}Ni_{0.5}Mn_{1.5}O_4$ spinel were studied at various C-rates and at different temperatures.

2. Experimental

A stoichiometric amount of lithium acetate [$Li(CH_3COO)\cdot 2H_2O$], manganese acetate [$Mn(CH_3COO)_2\cdot 4H_2O$], and nickel acetate [$Ni(CH_3COO)_2\cdot 4H_2O$], were dissolved in an appropriate quantity of distilled water at room temperature. The solution was stirred at 50 °C and the citric acid was added to the solution which acts as chelating agent in the polymeric matrix. The pH of the solution was adjusted to 7.0 by slowly dropping ammonium hydroxide drop wise and continued stirring for 4 h. The temperature of the solution raised to 80–90 °C and continued stirring till the solution turned into high-viscous gel. The resulted gel was dried at 80 °C for 24 h in a temperature controlled oven of an accuracy of ±1 °C. The $Li_{1.02}Ni_{0.5}Mn_{1.5}O_4$ precursor powder was ground to fine powder and calcined at 450 °C under oxygen flowing conditions with a constant heating followed by cooling rate at 4 °C min^{-1} to decompose organic constituents. The calcined powder was ground to a fine powder and re-sintered successively at 700, 750, 800 and 850 °C for 16 h under oxygen flowing conditions and heating and cooling rate was maintained at 2 °C min^{-1} and the accuracy of the furnace temperature is ±5 °C.

Phase purity of the $Li_{1.02}Ni_{0.5}Mn_{1.5}O_4$ was characterized by powder X-ray diffraction (Rikagu model rotaflux) using the Cu Kα radiation with a scan rate of 1° min^{-1}. The morphology and particle shape and their distribution of the $Li_{1.02}Ni_{0.5}Mn_{1.5}O_4$ powders, obtained at different temperatures, were examined by employing scanning electron microscopy (JEOL, JSM-6500F). Cyclic voltammetry measurements have been carried out using a two-electrode cell by employing a potentiostat (EG & G, model 273A) at ambient temperature. The CV measurements were performed in the potential range of 3.5–4.9 V at a scan rate of 0.02 mV sec^{-1}. Chemical compositions of the resulting powders were analyzed by an inductively coupled plasma-atomic emission spectrometer (ICP-AES).

The cathode slurry was prepared by mixing active material with carbon black, KS6 graphite and polyvinylidene fluoride (PVdF) used as a conducting agents and binder, respectively, in the weight ratio of 85:3.5:1.5:10. The solvent *N*-methyl pyrrolidinone (NMP) was used as a dispersing medium and stirred to obtain composite slurry. The resulted slurry was pasted on the aluminum foil with the help of doctor blade. The coated aluminum foil was dried at 120 °C for 2 h to evaporate the NMP solvent. The cathode film was thermally pressed and punched into circular discs. The cathode electrode films were preserved in an argon filled glove box to avoid oxidation effect by moisture or air. The coin cell was made using $Li_{1.02}Ni_{0.5}Mn_{1.5}O_4$ as a cathode, lithium (FMC) metal foil as an anode and 1.0 M $LiPF_6$ as in ethylene carbonate (EC):diethyl carbonate (DEC) (1:1) solvent used as an electrolyte. The polypropylene membrane was soaked in an electrolyte for 24 h prior to use. The entire coin cell assembly was carried out in an argon-filled glove box (Unilab, Mbruan) in which both the moisture and oxygen contents were maintained at less than 1 ppm. The charge and discharge measurements were carried out at different C-rates over the potential range of 3.5–4.9 V using Maccor battery tester.

3. Results and discussion

As mentioned in the introduction, the structure, morphology, and crystallinity have a direct influence on the electrochemical performance of the materials used in lithium-ion batteries. The synthesis method and the sintering conditions are the major factors to control the structure and morphology. Fig. 1 shows the XRD patterns obtained from the $Li_{1.02}Ni_{0.5}Mn_{1.5}O_4$ materials sintered at different temperatures ranging from 700 to 850 °C. The cell parameters extracted from the corresponding XRD patterns are shown in Table 1. All the diffraction peaks can be indexed based on the cubic spinel structure with a space group of $Fd\bar{3}m$, since no superlattice structure was observed (it can be confirmed from the plateau in capacity–voltage curve as well, see Fig. 4(b)) [26]. In this spinel-framework structure, the oxygen ions at the 32e sites form cubic-close packing and in which all the transition metals (Mn or Ni) and Li ions are occupied in the octahedral (16d) and tetrahedral (8a) sites, respectively. Traces of $Li_xNi_{1-x}O$ impurity peaks are observed in the XRD pattern of 700 °C-derived $Li_{1.02}Ni_{0.5}Mn_{1.5}O_4$ (Fig. 1) closely to the spinel characteristic peaks of the (3 1 1), (4 0 0), (3 3 1) and (4 4 0) reflections [32,33]. However, the impurity is no longer to be observed at elevating temperatures. Nevertheless, the preparation of pure phase of controlled stoichiometry of nickel and oxygen content in the $Li_{1.02}Ni_{0.5}Mn_{1.5}O_4$ powders is difficult [34] due to similarity in the ionic radii of Li and Ni ions. From our XRD pattern, the absence of (2 2 0) reflection indicates that no transition metal ions exist in the tetrahedral (8a) sites [35]. The average grain size of the $Li_{1.02}Ni_{0.5}Mn_{1.5}O_4$ powders was estimated using the Scherer's formula [36]. The average grain size was found to be 45–60 nm and the grain size increases with increase of temperature.

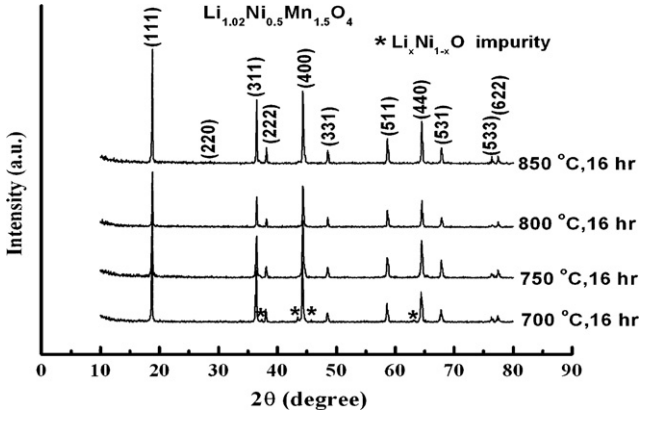

Fig. 1. X-ray diffraction patterns of $Li_{1.02}Ni_{0.5}Mn_{1.5}O_4$ powders sintered at different temperatures.

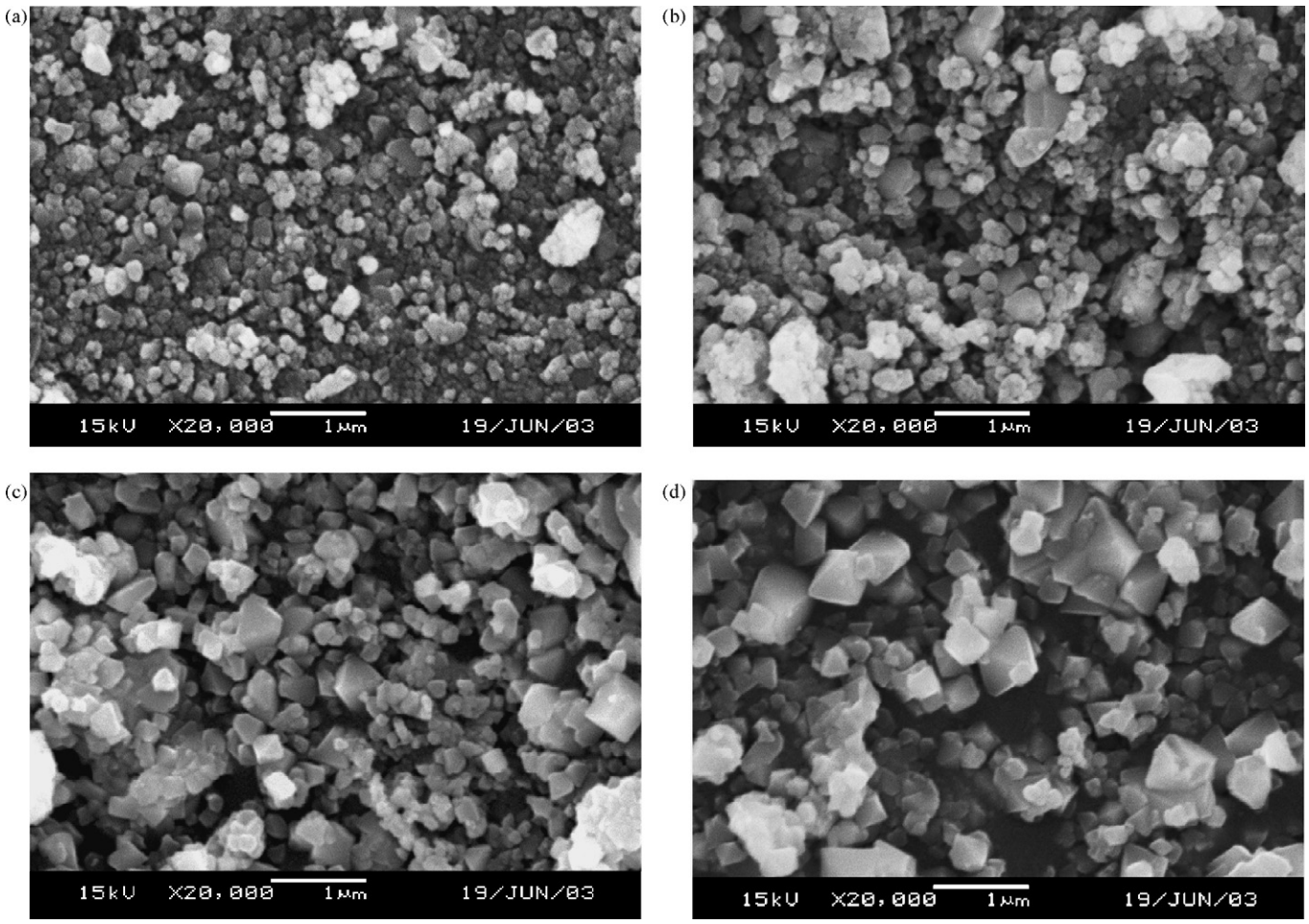

Fig. 2. SEM images of $Li_{1.02}Ni_{0.5}Mn_{1.5}O_4$ powders sintered at different temperatures: (a) 700 °C, (b) 750 °C, (c) 800 °C and (d) 850 °C.

Fig. 2a–d shows SEM images of the $Li_{1.02}Ni_{0.5}Mn_{1.5}O_4$ spinel powders sintered at 700, 750, 800 and 850 °C, respectively. It can be seen that the sintering temperature played an important role on the crystallinity of the material. The particle size increases with increasing sintering temperature. The average particle size of the samples sintered at 700 and 750 °C were found to be 0.1–0.3 μm and 0.2–0.3 μm, respectively. The samples sintered at 800 and 850 °C exhibits a more uniform particle size distribution and better crystallinity than the samples sintered at 700 and 750 °C. The average particle sizes were found to be 0.2–0.5 μm and 0.3–0.6 μm, respectively, for the samples sintered at 800 and 850 °C. In addition to phase purity, all the above-mentioned factors (particle size and particles size distribution) have a direct influence on the electrochemical performance of the materials.

Fig. 3 shows a typical cyclic voltammogram (CV) of the $Li_{1.02}Ni_{0.5}Mn_{1.5}O_4$ material in the voltage range from 3.5 to 4.9 V with a scan rate of 0.02 mV s^{-1}. As shown in Fig. 3, three reversible peaks can be observed in the CV curves at 4.02, 4.78, 4.82 V on charge and at 4.02, 4.60 and 4.65 V on discharge. The integrated area of low voltage 4 V peaks is much smaller than the high-voltage peaks around 4.8 V. In the case of $LiMn_2O_4$ spinel, the lithium-ion insertion and deinsertion occur at 4 V region with the redox pair of Mn^{3+}/Mn^{4+}. However, for $Li_{1.02}Ni_{0.5}Mn_{1.5}O_4$ spinel, all the Mn ions exist in +4 oxidation state and Ni ions exist in +2 oxidation state and occupy 16d sites instead of Mn^{3+} ions. The electrode potential of the $LiMn_2O_4$ could be shifted from 4.0 to 4.7 V by partial substitution of Mn ions with other transition metal ions. Dahn and co-workers have demonstrated the appearance of 4.7 V electrode potential regions by using ultra violet photoelectron spectroscopy [37]. The resulting Mn^{3+} leads to the formation of small peaks at around 4 V region and corresponds to the redox coupe Mn^{3+}/Mn^{4+} while the large peaks at around 4.8 V corresponds to the redox couple of Ni^{2+}/Ni^{3+} and Ni^{3+}/Ni^{4+}. Since all Ni exist in +2 oxidation state and all Mn exist in +4 oxidation state, the 4.0 V peaks are absent

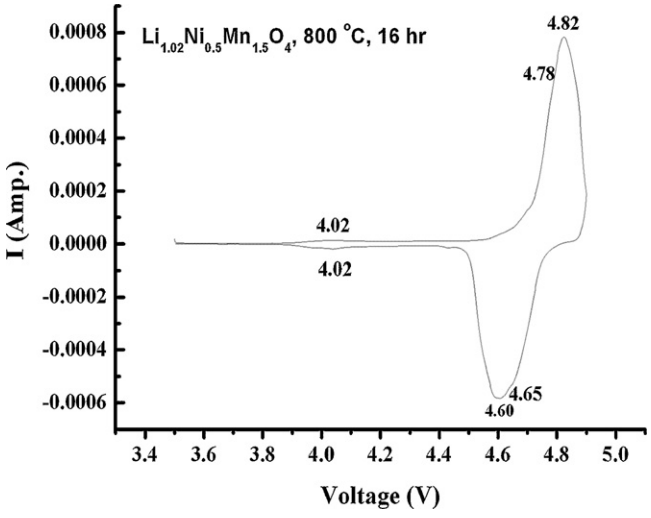

Fig. 3. Cyclic voltammogram of the $Li_{1.02}Ni_{0.5}Mn_{1.5}O_4$ spinel electrode sintered at 800 °C.

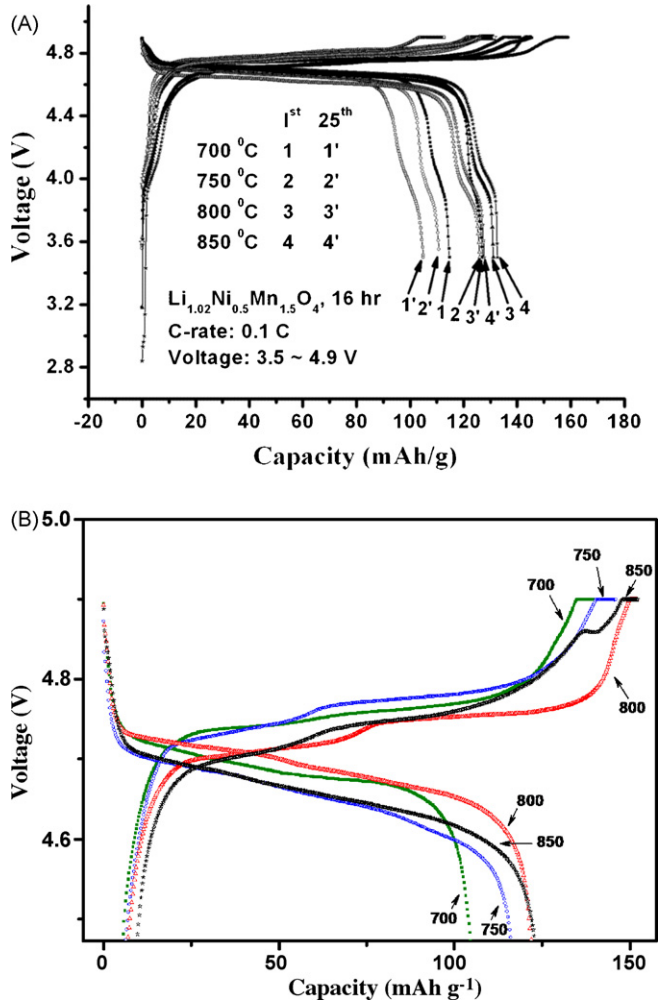

Fig. 4. Charge–discharge curves of $Li_{1.02}Ni_{0.5}Mn_{1.5}O_4$ electrode materials prepared at different temperatures under 0.1 C; (a) comparison of 1st and 25th cycles and (b) with a focus on the charge plateaus of the first cycle.

in the case of stoichiometric $LiNi_{0.5}Mn_{1.5}O_4$ spinel. The two peaks observed at higher voltage region for both charge and discharge are due to distinct redox voltages for Ni^{2+}/Ni^{3+} and Ni^{3+}/Ni^{4+} redox couples [38,39].

Charge and discharge measurements of the $Li_{1.02}Ni_{0.5}Mn_{1.5}O_4$ spinel cathodes were carried out in the potential range of 3.5–4.9 V at various *C*-rates and at different temperatures. The charging potential of 4.9 V (<5.0 V) has been selected in this work in order to avoid possible contribution of electrolyte reaction products to the electrochemical performance of the material. Fig. 4(a) shows the 1st and 25th charge/discharge profiles of the $Li_{1.02}Ni_{0.5}Mn_{1.5}O_4$ spinel materials sintered at 700, 750, 800 and 850 °C, for 16 h in the potential range of 3.5–4.9 V at 0.1 C. When increasing the charge and discharge cycles, the discharge capacity of the materials sintered at 700, 750, 800 and 850 °C, for 16 h decreases from 114.7, 127.1, 131.0, 132.6 mAh g^{-1} at the first cycle to 105.0, 124.7, 126.1, 127.6 mAh g^{-1} at the 25th cycle. The corresponding capacity retentions are of 93.1%, 95.8%, 96.5%, 97.2% at the 25th cycle and the results showed that the capacity retention increases with increasing temperature. The 1st cycle charge plateau regions for the $Li_{1.02}Ni_{0.5}Mn_{1.5}O_4$ synthesized at various temperatures are focused for better understanding their behaviors. From Fig. 4(b), it is found that only 700 °C-heated $LiNi_{0.5}Mn_{1.5}O_4$ shows one plateau, and rest of the samples (750, 800 and 850 °C-heated) show two plateaus. It

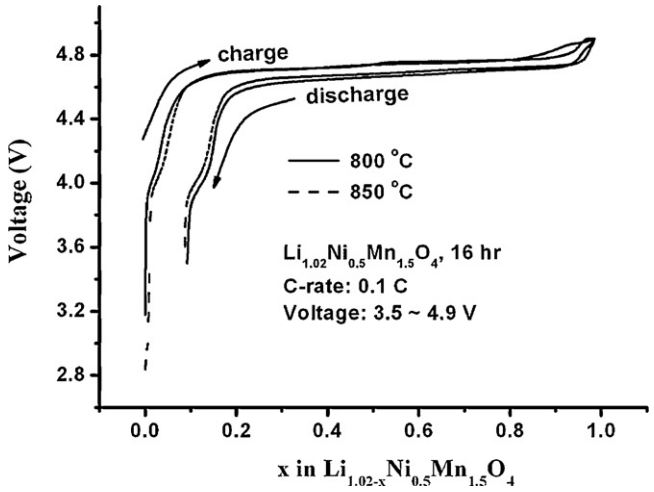

Fig. 5. Relationship between potential to degree of Li content in, respectively, 800 and 850 °C-heated $Li_{1.02}Ni_{0.5}Mn_{1.5}O_4$ electrode materials during charge–discharge process.

indicates the crystalline structure for 700 °C-heated $LiNi_{0.5}Mn_{1.5}O_4$ is primitive cubic $P4_332$ (cation ordering) and 750, 800 and 850 °C-heated ones are face-centered cubic $Fd3m$ (cation disordering). The behavior is identical to the literature reports [40,41]. The charge/discharge profile as a function of x for the $Li_xNi_{0.5}Mn_{1.5}O_4$ spinel materials sintered at 800 and 850 °C are presented in Fig. 5. Three voltage plateaus were developed in charge/discharge at 4.0 and 4.7 V regions. The charge–discharge curves agree well with the results obtained from CV, where the peaks in CV correspond to the voltage plateau in charge–discharge curves. As shown in Fig. 5, the discharge capacities of 131.0 and 132.6 mAh g^{-1} were obtained for the material sintered at 800 and 850 °C, respectively, which is almost 90% of its theoretical capacity (147.6 mAh g^{-1}).

To evaluate the rate capability, the charge and discharge measurements were carried out for $Li_{1.02}Ni_{0.5}Mn_{1.5}O_4$ material at 0.5 C in the potential range of 3.5–4.9 V and the results are presented in Fig. 6. As seen in this figure, the discharge capacities obtained for the materials sintered at 700, 750, 800 and 850 °C are 110.8, 127.2, 132.3 and 132.5 mAh g^{-1} at the first cycle and 103.6, 121.6, 123.8 and 125.9 mAh g^{-1} at the 25th cycle, respectively. The corresponding capacity retentions are of 97.4%, 98.2%, 98.5% and 98.7%

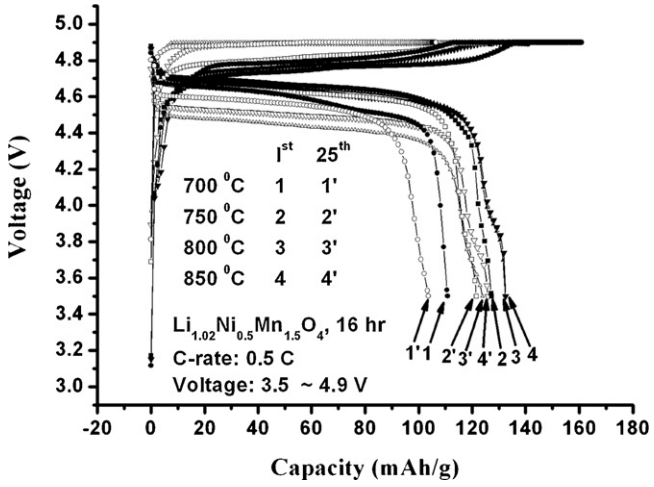

Fig. 6. Comparison of 1st and 25th charge–discharge curves of $Li_{1.02}Ni_{0.5}Mn_{1.5}O_4$ electrode materials prepared at different temperatures under 0.5 C.

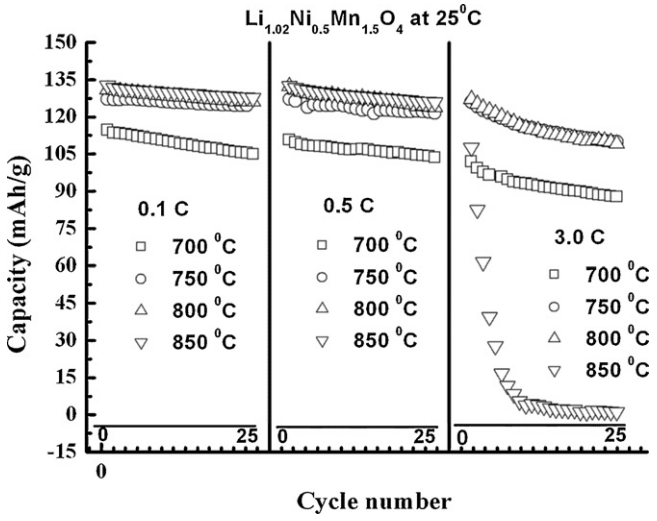

Fig. 7. Comparison of cycling performance of $Li_{1.02}Ni_{0.5}Mn_{1.5}O_4$ electrode materials prepared at different temperatures under different *C*-rates at 25 °C.

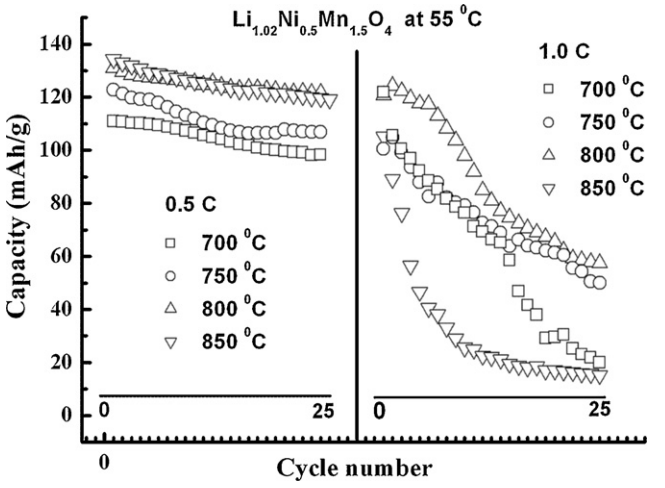

Fig. 8. Comparison of cycling performance of $Li_{1.02}Ni_{0.5}Mn_{1.5}O_4$ electrode materials prepared at different temperatures under different *C*-rates at 55 °C.

at the 25th cycle and the results showed that the capacity retention increases with increasing temperature. It can be seen that the materials sintered both at 800 and 850 °C shows a similar performance and exhibits a higher initial capacity and better capacity retention. The discharge capacities as a function of cycle number up to 25 cycles at different *C*-rates for the materials synthesized at different temperatures are shown in Fig. 7. As discussed above, at lower *C*-rates the materials sintered at 800 and 850 °C show better discharge capacity and capacity retention compared to the materials sintered at 700 and 750 °C. This result was attributed to good crystallinity as evidenced from XRD and SEM analysis. However, at higher *C*-rate (3.0 C), a drastic capacity fading was observed for the $Li_{1.02}Ni_{0.5}Mn_{1.5}O_4$ material sintered at 850 °C. The reason for fast capacity fading of the 850 °C-heated materials under high current density can be concluded to be higher internal resistance of the cell. It can be easily understand by considering capacity–voltage profile of 850 °C-heated $Li_{1.02}Ni_{0.5}Mn_{1.5}O_4$ at 0.1 and 0.5 C. The charge plateau is around 4.7 V at 0.1 C and is dramatically increased to around 4.9 V at 0.5 C. However, the behavior is not observed for low temperature-derived $Li_{1.02}Ni_{0.5}Mn_{1.5}O_4$. The possible reasons can be related to serious oxygen deficiency and the growth of the particle size for the $Li_{1.02}Ni_{0.5}Mn_{1.5}O_4$ synthesized at higher temperature (850 °C). Therefore, once the *C*-rate higher than 0.5 C, the plateau must rise higher than 4.9 V. Owing to the potential window limited up to 4.9 V, full charging state at higher *C*-rate (higher than 0.5 C) is not possible for 850 °C-$Li_{1.02}Ni_{0.5}Mn_{1.5}O_4$, so that lower capacity is obtained. The impurity for 850 °C-heated $Li_{1.02}Ni_{0.5}Mn_{1.5}O_4$ is not observed, which can only be seen for 700 and 750 °C-heated samples. Therefore it should not the reason for the poor capacity at 3 C.

In order to find high temperature performance of the $Li_{1.02}Ni_{0.5}Mn_{1.5}O_4$ material, the charge and discharge cycling were carried out at 55 °C at two different *C*-rates, namely, 0.5 and 1.0 C, and the results are shown in Fig. 8. The initial discharge capacities of 130.9 and 134.0 mAh g^{-1} were obtained at 0.5 C, respectively, for the materials sintered at 800 and 850 °C. However, at 1.0 C, the capacity retention of the materials sintered at 750 and 800 °C showed better performance than other materials. In contrast to the performance at 25 °C, the material sintered at 850 °C showed a drastic capacity fading at 55 °C. This poor cycle performance possibly due to structural damage caused by the undesirable reaction products formed from the electrolyte at high temperature.

4. Conclusions

Spinel $Li_{1.02}Ni_{0.5}Mn_{1.5}O_4$ materials were successfully prepared using a citric acid assisted sol–gel method at various sintering temperatures such as 700, 750, 800 and 850 °C. The electrochemical performance is highly dependent on the crystallinity, particle size and particle sized distribution of the materials. Although, a high degree of crystallinity can be achieved at high sintering temperature, it increases the particle size. Therefore, it is of great importance to find out an optimal sintering temperature to counterbalance formation of impurity phases, increasing crystallinity and growth of particles size. Among the materials prepared, $Li_{1.02}Ni_{0.5}Mn_{1.5}O_4$ prepared at both 800 and 850 °C delivered the highest specific discharge capacity and the best capacity retention at 0.1 and 0.5 C at 25 °C. However, the high temperature (55 °C) performance of the $Li_{1.02}Ni_{0.5}Mn_{1.5}O_4$ material prepared at 850 °C leads to a decrease in both capacity and capacity retention whereas the material prepared at 800 °C showed an excellent rate capability and cycling performance at 55 °C. The reason may be originated from the larger crystalline size as well as the serious oxygen deficiency of $Li_{1.02}Ni_{0.5}Mn_{1.5}O_4$ at high temperature treatment. However, with proper control of the synthesis process, it can be suggested that the $Li_{1.02}Ni_{0.5}Mn_{1.5}O_4$ material could be a promising high-voltage cathode material for an advanced high energy density lithium-ion batteries.

Acknowledgements

The support from National Science Council of Taiwan (Contract no: 96-ET-7-011-002-ET), National Synchrotron Radiation Research Center (NSRRC) and National Taiwan University of Science & Technology is gratefully acknowledged.

References

[1] P.G. Bruce, B. Scrosati, J.M. Tarascon, Angew. Chem. Int. Ed. 47 (2008) 2930.
[2] M.S. Whittingham, Chem. Rev. 104 (2004) 4271.
[3] A.S. Arico, P.G. Bruce, B. Scrosati, J.M. Tarascon, W. Van Schalkwijc, Nat. Mater. 4 (2005) 366.
[4] J.R. Dahn, U.V. Sacken, C.A. Michel, Solid State Ionics 44 (1990) 87.
[5] K. Mizushima, P.C. Jones, P.J. Wiseman, J.B. Goodenough, Mater. Res. Bull. 15 (1980) 783.
[6] M.M. Thackeray, W.I.F. David, P.G. Bruce, J.B. Goodenough, Mater. Res. Bull. 18 (1983) 461.
[7] Y. Xia, Y. Zhou, M. Yoshio, J. Electrochem. Soc. 144 (1997) 2593.
[8] C. Tsang, A. Manthiram, Solid State Ionics 89 (1996) 305.
[9] T. Ohzuku, M. Kitagawa, T. Hirai, J. Electrochem. Soc. 137 (1990) 769.
[10] J.M. Tarascon, D. Guyomard, Electrochim. Acta 38 (1993) 1221.

[11] D.H. Jang, Y.J. Shin, S.M. Oh, J. Electrochem. Soc. 143 (1996) 2204.
[12] R.J. Gummow, A. de Kock, M.M. Thackeray, Solid State Ionics 69 (1994) 59.
[13] D.H. Jang, S.M. Oh, J. Electrochem. Soc. 144 (1997) 3342.
[14] B.J. Hwang, R. Santhanam, D.G. Liu, J. Power Sources 102 (2001) 326.
[15] B.J. Hwang, Y.W. Tsai, R. Santhanam, D.G. Liu, J.F. Lee, J. Electrochem. Soc. 150 (2003) A335.
[16] Q. Zhong, A. Banakdarpour, M. Zhang, Y. Gao, J.R. Dahn, J. Electrochem. Soc. 144 (1997) 205.
[17] C. Sigala, D. Guyomard, A. Verbaere, Y. Piffard, M. Tournoux, Solid State Ionics 81 (1995) 167.
[18] A. Eftekhari, J. Power Sources 124 (2003) 182.
[19] H. Kawai, M. Nagata, H. Kageyama, H. Tukamato, A.R. West, Electrochim. Acta 45 (1999) 315.
[20] K. Amine, H. Tukamoto, H. Yasuda, Y. Fujita, J. Power Sources 68 (1997) 604.
[21] S.H. Park, Y.K. Sun, Electrochim. Acta 50 (2004) 431.
[22] J.H. Kim, S.T. Myung, Y.K. Sun, Electrochim. Acta 49 (2004) 219.
[23] M. Kunduraci, J.F. Al-Sharab, G.G. Amatucci, Chem. Mater. 18 (2006) 3585.
[24] M.M. Thackeray, C.S. Johnson, J.T. Vaughey, N. Li, S.A. Hackney, J. Mater. Chem. 15 (2005) 2257.
[25] K. Ariyoshi, S. Yamamoto, T. Ohzuku, J. Power Sources 119–121 (2003) 959.
[26] K. Ariyoshi, Y. Iwakoshi, N. Nakayama, T. Ohzuku, J. Electrochem. Soc. 151 (2004) A296.
[27] T. Ohzuku, K. Ariyoshi, S. Takeda, Y. Sakai, Electrochim. Acta 46 (2001) 2327.
[28] T. Ohzuku, S. Takeda, M. Iwanaga, J. Power Sources 81 (1999) 90.
[29] Y. Idemoto, H. Narai, N. Koura, J. Power Sources 119–121 (2003) 125.
[30] Y.K. Sun, Solid State Ionics 100 (1997) 115.
[31] B.J. Hwang, R. Santhanam, D.G. Liu, J. Power Sources 101 (2001) 86.
[32] K. Amine, H. Tukamoto, H. Yasuda, Y. Fujita, J. Electrochem. Soc. 143 (1996) 1607.
[33] J.H. Kim, S.T. Myung, C.S. Yoon, S.G. Kang, Y.K. Sun, Chem. Mater. 16 (2004) 906.
[34] S.T. Myung, S. Komaba, N. Kumagai, H. Yashiro, H.T. Chung, T.H. Cho, Electrochim. Acta 47 (2002) 2543.
[35] R. Alcantara, M. Jaraba, P. Lavela, J.L. Tirado, Ph. Biensan, A. de Guibert, C. Jordy, J.P. Peres, Chem. Mater. 15 (2003) 2376.
[36] B.D. Cullity, S.R. Stock, Elements of X-Ray Diffraction, 3rd ed., Prentice Hall, 2001, p. 170.
[37] Y. Gao, K. Myrtlc, M. Zhang, J.N. Reimers, J.R. Dahn, J. Electrochem. Soc. 144 (1997) 205.
[38] Y. Terada, K. Yasaka, F. Nishikawa, T. Konishi, M. Yoshio, I. Nakai, J. Solid State Chem. 156 (2001) 286.
[39] A. Van der ven, C. Marianetti, D. Morgen, G. Ceder, Solid State Ionics 135 (2000) 21.
[40] M. Kunduraci, G.G. Amatucci, J. Power Sources 165 (2007) 359.
[41] J.-H. Kim, C.S. Yoon, S.-T. Myung, Jai Prakash, Y.-K. Sun, Electrochem Solid-State Lett. 7 (2004) A216.